

Relative Flux Calibration of Keck HIRES Echelle Spectra¹

Nao Suzuki², David Tytler³, David Kirkman, John M. O'Meara, & Dan Lubin
Center for Astrophysics and Space Sciences;
University of California, San Diego;
MS 0424; La Jolla; CA 92093-0424

ABSTRACT

We describe a new method to calibrate the relative flux levels in spectra from the HIRES echelle spectrograph on the Keck-I telescope. Standard data reduction techniques that transfer the instrument response between HIRES integrations leave errors in the flux of 5 – 10%, because the effective response varies. The flux errors are most severe near the ends of each spectral order, where there can be discontinuous jumps. The source of these errors is uncertain, but may include changes in the vignetting connected to the optical alignment. Our new flux calibration method uses a calibrated reference spectrum of each target to calibrate individual HIRES integrations. We determine the instrument response independently for each integration, and hence we avoid the need to transfer the instrument response between HIRES integrations. The procedure can be applied to any HIRES spectrum, or any other spectrum. While the accuracy of the method depends upon many factors, we have been able to flux calibrate a HIRES spectrum to 1% over scales of 200 Å that include order joins. We illustrate the method with spectra of QSO 1243+3047 towards which we have measured the deuterium to hydrogen abundance ratio.

1. Introduction

In recent decades, the combination of large aperture telescopes and high resolution spectrographs have allowed for precision analysis of a variety of astrophysical objects. Echelle

¹Based on data obtained with the Kast spectrograph on the Lick Observatory 3-m Shane telescope and with the HIRES and ESI spectrographs at the W.M. Keck Observatory that is a joint facility of the University of California, the California Institute of Technology and NASA.

²E-mail: suzuki@ucsd.edu

³E-mail: tytler@ucsd.edu

spectrographs are the instrument of choice for high resolution, and most large telescopes now have one (Vogt 1987; Diego et al. 1990; Dekker et al. 2000; Noguchi et al. 1998; Tull 1998; McLean et al. 1998).

Echelle gratings can give spectra with high spectral resolution, with a large slit width, and a large wavelength range in a single setting (Schroeder 1987). An echelle grating disperses the spectrum into many tens of spectral orders, which are then cross dispersed by a second dispersive element so that the orders can be placed, one above the other, on a rectangular CCD detector. It is difficult to combine the spectra from the many spectral orders of an echelle to produce a single continuous spectrum. This difficulty arises because the response varies rapidly across each order, and at a given wavelength is usually different in different orders.

High quality relative flux calibration of echelle spectra is highly desirable in many scientific applications. For example, accurate flux levels over a large range of wavelengths makes it much easier to place continuum levels on spectra with pervasive blended absorption, such as the Lyman alpha forest absorption seen in high redshift QSO spectra.

In this paper, we discuss the relative flux calibration of spectra from the HIRES echelle spectrograph on the Keck-I telescope (Vogt et al. 1994). We do not discuss absolute flux calibration, as it requires additional calibration data and is not necessary for our absorption line work. We intend that a spectrum with relative flux calibration has the correct shape over some range of wavelengths, and differs from an absolute calibration in only the normalization.

We developed the methods described in this paper to improve our measurements of the primordial Deuterium to Hydrogen abundance ratio in QSO absorption systems, for which the bulk of our spectra come from HIRES. We have found that we obtain more accurate and reliable estimates of the absorption column densities when we use spectra with accurate relative flux. High quality flux calibration was not a major design goal for HIRES, and we have found that special steps must be taken to obtain the quality of calibration that we need for our work on D/H. The usual (Willmarth & Barnes 1994; Massey et al. 1992; Clayton 1996) methods of echelle flux calibration appear inadequate for reasons that we do not fully understand. This inadequacy motivated the development of the methods we describe.

We would like to both minimize the flux errors in our spectra, and to estimate the size of errors which remain after our calibrations. We shall find that the flux calibration errors depend on wavelength and they are correlated on various wavelength scales. We would like to estimate the size of the errors on these different scales. We would also like to make the error in the relative flux calibration less than the photon noise on some relevant scale. For example, when we fit a flat continuum level to a 50 pixel segment of a HIRES spectrum with

signal to noise ratio of 100 per pixel, the photon noise on the continuum level is 0.14%.

We found that is harder to approach a given accuracy in relative flux calibration in many places. These places include the regions where echelle orders join, regions where spectra have lower signal to noise ratio, wavelengths in the near UV, and in general as the wavelength range increases. It is very hard to get flux calibration errors of $< 1\%$ over even a wavelength range of $< 40 \text{ \AA}$ within one HIRES order. Fortunately for our absorption line work, errors that vary smoothly over wavelength scales $> 40 \text{ \AA}$ are not as serious as smaller scale errors.

In this paper, we describe a way of calibrating the relative flux in a HIRES spectrum using well calibrated reference spectra of the same target to transfer flux information from other spectrographs to the HIRES spectra. We force each HIRES spectrum to have the shape of these reference spectra. This method should correct a variety of flux calibration errors, both from variable vignetting and differences in spectrum extraction and reduction. The method could also be applied to spectra from various spectrographs, and not just echelles. This method is based on that introduced by Burles & Tytler (1997, 1998) and applied with improvements to HS 0105+1619 in O’Meara et al. (2001).

The paper is organized as follows: we first describe the nature of inconsistencies between repeated HIRES observations of a target, and how this impacts flux calibration. Second, we describe the spectra we used to illustrate our flux calibration method. Third, we describe at first in overview, and then in detail, our methods for flux calibration. Fourth, we describe how we combine the HIRES orders that we have flux calibrated individually. Finally, we discuss the accuracy and errors of our method.

2. Description of the HIRES flux calibration problem

The usual methods of flux calibration appear inadequate when applied to HIRES spectra. When we determine the instrument response by observing a spectrophotometric standard star, different exposures of the same star give different instrument response functions, even when we believe that the exposures were taken with the same instrument configuration. For example, in Figure 1, we show the signal extracted from two HIRES integrations of G191-B2B. The exposures were taken on consecutive nights, with similar instrument configurations. On the second night the star was 0.07 degrees higher in the sky and the image rotator (Appendix B) physical angle differed by 0.071 degrees to compensate for the change in parallactic angle. The spectra were both extracted with Tom Barlow’s MAKEE software (April 2001 version). We show the “raw” ADU from the CCD before division by the flat field integration or any other calibration.

The differences between the two exposures shown in Figure 1 are large and unexpected. In particular, even though the exposures were taken on different nights, we did not expect to see large ($\sim 10\%$) differences within a single order, even after the two exposures were normalized to have the same mean flux in that order. The differences are largest ($\sim 10\%$) at the ends of the order. Similar differences (both in shape and magnitude) are present in each observed spectral order. However, the form of the difference is not precisely the same for each order, as demonstrated in Figure 2. Barlow & Sargent (1997) also noted the possibility of systematic flux errors of 10% near order overlaps.

Flux differences have also been reported for the Subaru telescope HDS echelle spectrograph that sometimes shows 10% changes during observations (Aoki 2002).

We have examined approximately 20 other pairs of standard star integrations from HIRES that have similar instrumental setups. Most show differences of order 10%, though the exact shape of the differences is not always the same. In addition to the “U” shaped ratios (seen in Figure 1), we see three other shapes for ratios: near flat ratios, tilted and ogive (or “fallen S”) shapes. In each case, the shapes of the ratios vary gradually order-to-order in a systematic way, such that adjacent orders have similar shapes. The shapes of the ratios vary much more between pairs of integrations than they do from order-to-order for a given pair of integrations.

Approximately 30% of integration pairs give flat ratios that indicate that the instrumental response was very similar for the two integrations, which should make flux calibration simple. A cursory examination did not show any predictors (e.g. telescope elevation, rotator angle, position of target on the slit, seeing) as to which pairs would be similar and which different.

In Figure 3, we show HIRES integrations on two stars that we flux calibrated in the usual manner, each using a response function determined from a HIRES exposure of a standard star. The spectra that we calibrated differ from the known flux levels by large amounts over a wide range of wavelengths. The main deviations are systematic across each HIRES order. We also see large differences at the order overlap wavelengths. Different ways of combining spectral orders leave different flux calibration errors. If we take the mean of the signals then the flux will jump in a single pixel, by up to 10%, where each order begins and ends. There will be approximately 70 such jumps in a complete HIRES spectrum with 36 orders.

In the past, we have attempted to reduce the flux errors by fitting continua to each order, and dividing by these continua, before we take the mean flux in a wavelength overlap. This method is unsatisfactory because it is very hard to ensure that the continua that we fit to adjacent orders have both the same flux levels and the same shapes, and we loose flux

information.

For some unknown reason, long integrations on a QSO show smaller differences than short integrations on a bright star. A dependence on integration time might relate to some averaging, perhaps related to the target position on the slit. A dependence on brightness might relate to the 100 times lower signal in the QSO integrations, and perhaps subsequent differences in the spectrum extraction. We still have difficulty flux calibrating QSO exposures, even though they appear to be more stable than exposures on standard stars, because usual procedures still require that we determine the instrument response from a standard star exposure.

The variations we see in standard star exposures indicate that there is some instability in either Keck+HIRES, in our data reduction processes, or in both. We have investigated two possible origins for the instability: variable vignetting inside of HIRES, and inadequate the extraction of the spectra. We do not see a clear signature of either in our spectra, but we do know that the vignetting is expected to change.

We have explored the possibility of extraction errors by varying the type of profile used during extraction, and the profile width, but found no differences from the standard extraction results from MAKEE. We also measured flux ratios from the raw counts in the CCD images that were similar to those in the spectra extracted by MAKEE.

We know that the vignetting inside HIRES changes with the position angle of the sky image on the HIRES slit and with the telescope elevation (Appendix B). When the image rotator is used there are two main options. We can use the image rotator in “Vertical angle mode” to keep the vertical angle along the slit, so that the position angle varies with the position of the target in the sky. The rotator can also be used to keep a desired position angle along the slit. If the rotator is not used, the relevant angle is the telescope elevation. The variation in vignetting arises from a known mechanical and optical misalignment between the Keck-I telescope and HIRES, and the expected amount of change in the vignetting, from ray tracing kindly provided by Steve Vogt, is approximately 10%, consistent with our observations.

We can account for why the ratios of HIRES spectra have similar shapes across all orders if the variable vignetting happens after the echelle, and before leaving the cross-disperser. In this part of HIRES the light from the red end of each order is separated from that in the blue end, but all orders are coincident. We might explain the shape of the ratios, and the similarity from order-to-order, if a varying amount of light misses the top and bottom of the cross-disperser (the grooves are vertical), where the red and blue ends of the orders land. This variation could arise when the cone of light from the telescope tips up and down in the

vertical plane that connects the center of the tertiary mirror and the HIRES slit.

However, we suspect that vignetting is not the sole cause of the variations in the flux, because we have seen variations in spectra taken under apparently identical instrumental conditions (same elevation, image rotator setting, and target location on the slit) on consecutive nights, as we saw in Figure 1.

The changes might also come from differences in the extraction of the spectra from the CCD image, e.g. if we do not extract a fixed proportion of the flux recorded at each wavelength. Differences in the extraction of spectra, including multiple integrations on a given target, are likely whenever there are changes in conditions, such as the location of the target along the slit, the seeing, the sky brightness and the amount of signal recorded. However, extraction problems seem an unlikely explanation for standard stars that have high signal to noise ratio.

3. Spectra we will use to Illustrate our Method

Here, we introduce the spectra that we will use to illustrate our method of relative flux calibration. This is the set of spectra that we used to measure D/H towards QSO 1243+3047 ($z_{em} = 2.64$, $V=16.9$; Kirkman *et al.* 2003). For our D/H work, we were mostly interested the flux calibration in a 40 Å region centered on the damped Ly α line near 4285 Å, and on the Lyman limit near 3210 Å. We began the development of the methods using a similar set of spectra of HS 0105+1619 that we had used to make an earlier D/H measurement (O’Meara *et al.* 2001).

We used 5 spectra from the Kast spectrograph on the Lick 3-m telescope, and one from the ESI echelle spectrograph on the Keck-II telescope. We used both the Kast and ESI spectra separately to make independent flux calibrations of 8 integrations from HIRES. Further details of the observations, including the dates, the resolution, the mean S/N, and plots of the spectra are in Kirkman *et al.* (2003). All of the spectra that we used were shifted into the heliocentric frame, and placed on a logarithmic wavelength scale with a constant velocity increment per pixel, although with different increments for different spectra.

3.1. Spectra from Kast

The Kast double spectrograph uses a beam splitter to record blue and red spectra simultaneously in two cameras. For QSO 1243+3047 we have five KAST integrations, one from 1997, and two each from 1999 and 2001. All integrations were obtained using the d46

dichroic that splits the spectrum near 4600 Å, the 830 line/mm grism blazed at 3460 Å for the blue side, and the 1200 line/mm grating blazed at 5000 Å for the red side. We reduced all exposures with the IRAF package `longslit`.

3.2. Spectra from ESI

ESI covers from 3900 – 11,000 Å in ten overlapping orders (Epps & Miller 1998; Bigelow & Nelson 1998; Sheinis et al. 2000). We have one exposure of QSO 1243+3047 using a 1” slit, taken in the echellette mode on January 11, 2000. From the same night, we also have an exposure of the flux standard star Feige 110.

3.3. Spectra from HIRES

Our HIRES spectra of QSO 1243+3047 all used similar instrumental setups. The angle of the HIRES echelle was the same for all exposures, and placed the center of each order near the center of the CCD. The cross-disperser angle was also similar for all exposures, except for one exposure that extended to much larger wavelengths. The image rotator (Appendix B) was used in vertical mode, to minimize slit losses from atmospheric dispersion. We used the C5 decker, which provides an entrance aperture to the spectrograph with dimensions 1.15” × 7.5”. In each case we placed the target near the middle of the slit. The spectra were all recorded on the engineering grade Tektronix CCD with 2048 × 2048 pixels that has been used in HIRES since 1994. The HIRES pixel size is 2.1 km s⁻¹.

The CCD is large enough to record beyond the free spectral range for all orders at wavelengths < 5200 Å, and we placed the spectra on the CCD such that we did record this flux for all such orders. All but one integration covered from near 3200Å out to 4700Å in approximately 36 orders. These integrations were 7200 – 9000 seconds long. The S/N in each integration is near 3 per 2.1 km s⁻¹ pixel near the Lyman limit at ~ 3200 Å, and rises to near 35 at the peak of the Lyα emission line at ~ 4400 Å.

The HIRES spectra we use are the normal output from the MAKEE software, which are the raw counts spectrum divided by spectra extracted from flat field integrations. In addition, the CCD defects were marked with negative error values. These spectra differ from the raw counts that we discussed in the previous section in that the flat field division has removed most of the variation across the orders due to the blaze and vignetting. Although this flat field division may introduce additional undesirable changes in the relative flux, we proceed with these spectra because it is imperative that the CCD defects have been removed.

3.3.1. HIRES Spectral Resolution

We measured the instrument resolution of HIRES by fitting Gaussian functions to narrow, apparently un-blended lines in a single Thorium-Argon arc integration taken before one of the QSO integrations. We fit hundreds of arc lines in all parts of the spectrum, and found a dispersion of $\sigma = 3.4 \pm 0.1 \text{ km s}^{-1}$, which corresponds to a FWHM spectral resolution of $8.0 \pm 0.2 \text{ km s}^{-1}$ ($b_{ins} = \sqrt{2}\sigma = 4.81 \pm 0.14 \text{ km s}^{-1}$). We did not detect any variation in the resolution with wavelength. However, we did detect that the arc lines are not Gaussian in shape, with more extended wings, such that the best fitting σ increases when we extend the fitting range around an individual line. We also expect that the spectra will have slightly different FWHM from the arc spectra, because the illumination of the slit is different. The wavelength shifts that we describe in the next section suggest that the resolution will depend in part on the guiding and seeing.

3.3.2. HIRES Wavelength Shifts

We measured wavelength shifts between the HIRES integrations and we shifted the spectra onto the same scale to correct these shifts. We measured the cross-correlations between each of the 7 integrations with the eighth that we used as the reference. An example of the shifts is shown in Figure 4. Comparisons of other pairs of integrations often show a much larger dispersion in the measured shifts. In all cases, the shifts measured in each order are consistent with a single shift for each integration. The shifts had a standard deviation of 0.7 km s^{-1} , which is 30% of one HIRES CCD pixel. Each shift was measured to an accuracy of 0.13 km s^{-1} , which we determined from the scatter in the shifts that we measured separately for each order.

These shifts may arise from differences in the placement of the QSO light in the HIRES slit, which projects to approximately 4 HIRES pixels. The 0.7 km s^{-1} rms shift is approximately 9% of the FWHM resolution, which itself is similar to the slit width. The shifts do not correlate with hour angle or the correction that was applied for the Earth’s orbital motion ($< 30 \text{ km s}^{-1}$) and spin ($< 0.4 \text{ km s}^{-1}$). The shifts are also larger than we expect from wavelength scale errors. However, we did find much larger wavelength scale errors when we did not ensure that MAKEE used enough arc lines to determine the dispersion solution for each order.

4. Overview of the Method

There are three main steps in our procedure to apply relative flux calibration to HIRES spectra.

- Step 1: Flux calibrate a high quality reference spectrum of the target.
- Step 2: Flux calibrate the HIRES echelle orders with the reference spectrum. This imposes the long scale ($> 10 \text{ \AA}$) spectral shape of the reference spectrum upon each HIRES echelle order. The flux information on smaller scales (e.g. absorption line profiles) still comes from HIRES.
- Step 3: Combine the HIRES orders. We first sum the integrations and then join the orders to give one continuous spectrum.

These procedures do not replace standard CCD spectrum extraction procedures. Rather, they should be thought of as a “software patch”, applied to correct errors that remain after the spectra have been extracted, and perhaps calibrated, in the usual way. Reasonably well calibrated HIRES spectra are required as inputs to our method, because the flux information on scales $< 10 \text{ \AA}$ will still come directly from the HIRES spectra. The procedure is not unique, and we expect that other sequences might be appropriate for different spectra.

We now discuss in further detail each of the steps outlined above.

5. Step 1: Flux Calibrating the Reference Spectra of the Target

Since we can not transfer information about the instrument response between exposures, we must “self-calibrate” each exposure we take with HIRES. The first step of our method is thus to obtain a well calibrated spectrum of the target. The reference spectrum must come from a well calibrated and stable spectrograph. In our work on Q1243+3047, we obtained reference spectra from both Lick+KAST and Keck+ESI, and compared them to gauge the accuracy of the final flux calibration.

5.1. Flux Calibration of Kast Spectra

To calibrate the flux in our Kast spectra of QSO 1243+3047, we took flux information from a model spectrum of G191 B2B for the 1997 spectrum, and a STIS spectrum of

BD 28 4211 for the 1999 and 2001 exposures. We discuss the reasons behind our choice of these standard stars in Appendix A. We measured and matched the resolution of the observed and reference spectra of the standard stars before we used them to calculate the Kast response function. The dip in the response at the end of blue CCD and the beginning of red the CCD is due to the changing efficiency of the beam splitter. In Figure 5, we illustrate the flux calibration process.

The spectrum shows atmospheric ozone absorption lines (Schachter 1991) as the wiggles of the raw CCD counts (panel b) below 3400 Å. Their strength depends on the temperature of the ozone layer and the effective airmass of the integration, and we have not made appropriate adjustments. We left the wiggles un-smoothed in the response (Figure 5, panel d) to help partially remove their effect from the quasar spectrum.

In Figure 6, we show the accuracy of the flux calibration of a Kast spectrum of another star. The flux residuals between our calibrated KAST spectrum and a STIS spectrum of the same star are less than 3%.

5.2. Flux Calibration of ESI Spectrum

We flux calibrate ESI spectra in the same way we do those from Kast. In Figure 7, we show the steps in the flux calibration of an ESI spectrum. The ESI orders overlap in wavelength, and in Figure 8, we see that the orders do not always have the same flux. These differences increase in size as we approach the end of an order. We have not investigated the origin of these flux differences. We cut off most of the regions where the differences exceeds 2% (which is the noise level in our spectrum) without leaving any gaps in the wavelength coverage. We do not know the size of the remaining error, especially in regions where there was no wavelength overlap, because we do not have redundant observations of bright stars. Nonetheless, the ESI spectra could have better relative flux calibration than HIRES spectra, for several reasons. ESI has fewer orders, each of which covers more wavelength range and a much larger portion of each order is sampled by adjacent orders. ESI has a fixed instrumental configuration and our ESI spectra have much higher S/N than our individual HIRES integrations, which may change the proportion of the flux that is extracted.

5.3. Errors in the Reference Spectra

The errors in the relative flux calibration of the reference spectrum are a fundamental limitation on how well we can apply relative flux calibration to the HIRES spectrum. One

way to explore these errors is to compare different reference spectra. We will see that the differences increase with wavelength range and they are the main source of error in our calibration of our HIRES spectra of QSO 1243+3047.

We found that the 5 Kast spectra show two types of shape. The two from 1999 are similar, as are the two from 2001. We call the sum of the two flux calibrated spectra from 1999 K99, and the two from 2001 K01. KSUM is our name for the sum of all five spectra. The 1997 spectrum is similar to K01, but has much lower S/N.

These two groups, K99 and K01, differ in shape on the largest scales across the whole Lyman- α forest, but they do have very similar shapes across a few hundred Angstroms after we normalize them to each other at those wavelengths. These differences are best seen when we smooth them slightly by differing amounts to reduce differences in the spectral resolution. The K01 spectra have up to 10% systematically higher flux at wavelengths $< 3400 \text{ \AA}$ than do the K99 spectra. The K01 spectra had a few percent lower flux from $4000 - 4300 \text{ \AA}$ and higher flux across the Ly α emission line. We do not know the origin of these differences. Possible origins include variation in atmospheric extinction (Burki et al. 1995) or a variation in the QSO.

We find that the ESI spectra differed from the various Kast spectra by typically 2% or less per Kast pixel, from $4100 - 4400 \text{ \AA}$. The differences correlate over a few Kast pixels in the Lyman- α forest, with no large scale trends, except that to the red side of the Ly α emission line the ratio of the Kast to ESI flux increases by approximately 5% from $4300 - 4400 \text{ \AA}$ for all five Kast spectra.

6. Step 2: Flux Calibrating HIRES Echelle Orders with a Reference Spectrum

We calibrated the relative flux in a HIRES spectrum using a calibrated reference spectrum from either Kast or ESI. We divided a smoothed version of the HIRES spectrum by the reference spectrum to find the “Conversion Ratio” spectrum. We found that the smoothed HIRES spectrum and the reference had to have the same wavelength scale and resolution, because the Lyman- α forest absorption lines cause the flux to vary rapidly in wavelength. We calibrated the individual orders of each HIRES integration using a smooth function fitted to the conversion ratio spectra, one for each order of each integration.

In Figure 9, we illustrate the calibration of the relative flux in the HIRES orders that we describe in the following five sub-sections.

6.1. Wavelength Matching

Because the wavelengths from HIRES are more accurate, we shifted the Kast spectra onto the HIRES wavelength scale. We measured the shifts by cross-correlation of complete HIRES orders, and we confirmed the values by cross-correlating individual strong lines in the Lyman- α forest.

Some of the wavelength shifts may arise because the QSO was not exactly centered in the slit. This is a reasonable explanation for the typical shift which was 42 km s^{-1} , or 0.4 Kast pixels, only 17% of the projected width of a 2 arcsecond wide slit. These shifts should vary monotonically along a spectrum, and some Kast spectra show this. However, Figure 10 shows that other spectra have more complex wavelength shifts. In such cases we measured the mean shift for each HIRES order, and we fit a low order polynomial to these mean values, similar to that used to fit the arc line wavelengths, to give a smoothly changing wavelength scale without gaps or discontinuities.

We also placed the ESI spectra on the HIRES wavelength scale. This wavelength scale assignment was obtained by first smoothing the HIRES spectra to the approximate spectral resolution of ESI, and then finding the velocity shift by cross-correlation of the ESI with the HIRES integration. We shifted the complete ESI spectrum by $+5.61 \text{ km s}^{-1}$, which is 7.5% of the projected 1 arcsec slit width. As with the Kast spectra, this shift is larger than we would expect from the wavelength fits to the arc calibration lines and may arise because the QSO was not exactly centered in the slit.

6.2. Resolution Matching

We smooth the HIRES spectrum to match the resolution of the Kast spectrum. This procedure is sensitive to wavelength shifts between the two spectra, and hence it was done after the wavelength scales were matched. In contrast, the wavelength scale matching is insensitive to the spectral resolution. We smoothed the HIRES spectrum, and sampled it in the wavelength bins of the Kast spectrum. We smoothed with a Gaussian function of known FWHM, truncated at 2σ , and normalized to unit area. We smoothed by different FWHM to find the amount of smoothing that left the smallest residuals between the smoothed HIRES and Kast spectra. These residuals appeared flat across strong absorption lines, which suggests that a Gaussian is an adequate approximation to the line spread function of the Kast spectrum. As with the wavelength matching, the Lyman- α forest provides additional signal for resolution matching.

The Kast spectral resolution varies from spectrum to spectrum, and it can vary with

wavelength in a spectrum, depending on where we chose to focus. We took the Kast resolution to be the FWHM of the smoothing applied to the HIRES, after subtracting the initial HIRES 8 km s^{-1} FWHM in quadrature. For example, in the 1999 spectra of QSO 1243+3047, the FWHM of the Kast spectrum is near 300 km s^{-1} near 3300 \AA and from $3800 - 4300 \text{ \AA}$ but it improves to 220 km s^{-1} near 3500 \AA , where the measurement error is approximately $10 - 30 \text{ km s}^{-1}$, depending on the region of the Lyman- α forest. We smoothed the HIRES spectrum by a single mean FWHM even when the resolution varied along the Kast spectrum. Using similar methods we found that the ESI spectrum had a FWHM of $63.2 \pm 3.0 \text{ km s}^{-1}$.

6.3. Calculating the Conversion Ratio

We divide the smoothed HIRES spectrum by the Kast spectrum, to obtain the “conversion ratio” (CR) spectrum. The Lyman- α forest hinders our calculation of the CR, because we are very sensitive to slight remaining errors in the wavelengths and the resolution. When we calculate the CR, we weight the flux in the individual spectra by their errors, and we assign an error to each pixel in the CR. It is common to see increased error in the CR near strong absorption lines (e.g. near 4285 \AA in panel (e) of Figure 9), but this error does not have a systematic shape when the wavelengths and resolution are well matched.

6.4. Smoothing the Conversion Ratio

We fit the CR spectra to obtain a smoothly changing function. The original CR spectra vary from pixel to pixel because of photon noise in the reference and HIRES spectra, especially in strong absorption lines. These variations can be much larger than the expected change in the flux calibration and hence we can improve the flux calibration by interpolating. We explored various ways of smoothing and fitting, some in one dimension, along each order separately, and others in two dimensions, both along and between adjacent orders. The best choice will increase the S/N in the CR as much as possible without changing the structure.

We found that a 4th order Chebyshev polynomial fit to the CR spectrum for each HIRES order was a good choice. We choose this order by trial and error. It leaves enough freedom to fit the shapes of the CR and give a reduced $\chi^2 \simeq 1$. Other fits would be appropriate in spectra with different amount of structure and S/N. In Figure 11, we show the CR spectra for many HIRES orders. We see that the CR spectra for adjacent orders are very similar in shape, but change systematically as we move across many orders. We also found that the

changes in shape from order-to-order are larger than those between integrations for a given order, except for the effects of photon noise in the CR.

We calculate the CR twice, in an iterative fashion, to improve the accuracy near the ends of the HIRES orders. The first time, we stop the calculation before the order ends, where the filter, which we use to smooth the HIRES spectrum to the resolution of the reference spectrum, just touches the last pixel in the order. We can not, at that time, calculate the CR for the remaining pixels because we do not know the flux from beyond the end of the order. This flux is needed when we smooth the HIRES spectrum to match the reference spectrum. We do, however, allow the fit to the CR to extrapolate to the end of the order, and we use that extrapolation to make the first estimate of the flux calibration. When we calculate the CR the second time, we know the HIRES flux from beyond the end of the order, because we have already calibrated the whole HIRES spectrum.

An example of the type of error that can occur in the CR at order ends is shown in Figure 12. In middle panel on the left, the CR is erroneously low in the first two pixels at the start of order 98. Here we calculated the CR once only, and we ignored the flux from beyond the end of the order, where there happens to be a $\text{Ly}\beta$ absorption line. This absorption line lowers the flux in the reference spectrum, but not in the HIRES spectrum for that order.

The error in the relative flux calibration of a HIRES integration depends in part on the S/N in that HIRES integration. The conversion ratios in Figure 12 are for a second integration of QSO 1243+3047 that can be compared to the integration shown in Figure 11. The two integrations were calibrated using the same Kast spectrum, and hence the differences are caused by noise in the HIRES integration, especially at the shortest wavelengths.

We experimented with other ways of smoothing the CR to reduce the effects of photon noise. The 4th order polynomials smooth in wavelength along an order, but they do not use any information from adjacent orders. We made a 2-dimensional map of the CR in the coordinate frame of the HIRES CCD detector, and we smoothed this map in both dimensions, both using a Gaussian filter and independently by fitting a 2D surface using Chebyshev polynomials. The Gaussian filter did not work well because the largest width that did not change the shape of the CR surface had a 4σ width of only 3 orders, not enough to reduce the noise significantly. In Figure 13, we show a surface fit that was an improvement over the 1D polynomial fits, but we did not use this in Kirkman et al. (2003).

The error in the CR depends on the S/N in each CR pixel, and on the fitting or smoothing that we use. The error will correlate on the smoothing scale. When we apply a 4th order polynomial to each order of 40 \AA , (the correlation length is approximately 10 \AA) and this can be seen when we compare Figures 11 & 12. There are also strong correlations

in the CR near the ends of orders, and near strong absorption where the errors are largest.

The contribution to the error in the CR from the S/N in the reference or HIRES spectra can be estimated from the number of pixels in the correlation length. There are approximately 34 pixels in a Kast spectrum per HIRES order, and hence 8.5 per correlation length. An individual Kast spectrum of QSO 1243+3047 has S/N 60 per pixel near 4250 Å and 20 near 3250 Å. The CR will then have errors of at least 0.6% near 4250 Å and 1.7% near 3250 Å.

6.5. Applying the Conversion Ratio

We divide the original HIRES integration, with full spectral resolution and pixels, by the 1D fits to the CR to obtain the desired flux calibrated HIRES spectrum. Since we have not merged the orders, the wavelength overlaps remain. The resulting HIRES integration now has relative flux calibration on each order.

7. Step 3: Combine the HIRES Orders

The final step is to combine the fluxed HIRES orders into a single spectrum. We add the HIRES integrations that have very similar wavelength coverage, order by order, and then merge the orders. We choose this sequence because it facilitates checks of the relative flux calibration. We compare the flux in each order in multiple integrations before we sum the integrations. After they are summed, the enhanced S/N makes it easier to see errors in the flux calibration in the wavelength overlap between orders.

First, we place all orders from all HIRES integrations on a single wavelength scale, so that pixels from orders that overlap in wavelength sample exactly the same wavelengths. We choose a scale with a constant velocity increment of 2.1 km s⁻¹ per pixel, equivalent to constant log wavelength increment. This choice has two advantages over constant wavelength: in velocity units, the spectral resolution of the echelle does not vary significantly with wavelength, and we use velocity units to describe the widths of absorption line systems.

We simultaneously correct errors in the wavelength scales, using information from the cross-correlation of different integrations as discussed in (§3.3.2). We do this correction at the same time because we want to re-bin the HIRES spectra only once.

We calculate the mean flux in each pixel, from all integrations, after rejecting large deviations that we identify by evaluating the χ^2 statistic for each pixel. We ignore the flux

in a pixel from an individual integration if it is $> m\sigma_i$ away from the weighted mean for all integrations, where σ_i are the errors on the fluxes in the individual integrations. The value of m was determined iteratively to remove most pixels with conspicuously deviant flux values. For QSO 1243+3047, we use $m = 2$. The algorithm iterates, and re-derives the χ^2 after rejecting the flux value from one integration. If all integrations are $> m\sigma$ away from the weighted mean, we examine the errors. If the errors in some of the integrations have data, shown by non-zero errors returned by MAKEE, we use the flux from the integration with the smallest error as the mean. If, however, there is no data in a particular pixel, for example because of a known CCD defect, then we use the weighted mean of the two pixels on either side, again using only those integrations that are within $m\sigma$ of the weighted mean for that wavelength. If none of the above criterion are met, we use the average of the fluxes in all integrations.

Finally, we verify that adjacent orders show similar flux levels where they overlap, and we used a weighted mean to combine the orders in these regions, producing a single flux calibrated spectrum. In Figure 14, we show order overlap for spectra of star Feige 34. This spectrum can be compared to the spectra in Figures 3 that show the flux calibration using usual methods. The ratio of the flux in adjacent orders shows most variation near 3250 Å : 0.92 – 1.08%, and decreases to 0.98 – 1.02 near 4300 Å, where the signal to noise ratio is highest in the Kast spectrum that we used as a reference. The calibration of Feige 34 used the method and algorithm that we developed and applied to our spectra of QSO 1243+3047, with a few exceptions. The star does not have Lyman- α forest lines, and hence we matched the wavelength scale of the Kast and HIRES spectra using a single shift for the whole Kast spectrum. We fitted the CR with one 4th order polynomial per order. A 6th order fit would work better near 4300 Å where the signal to noise ratio is high.

We consistently found, from many spectra, that the remaining difference between the orders was largest at the end of an order, where the CR is less well known. Hence, we tapered the flux from each order using a weighting function that declined linearly from one, where the overlap begins, to zero, where the order ends.

8. Comparison of Spectra of QSO 1243+3047 Calibrated with Different Reference Spectra

We made several different calibrations of the HIRES spectra of QSO 1243+3047 using different low resolution spectra to convey the flux information. We label these HIRES spectra by the spectra that we used for the flux calibration: hence, HK99 is the HIRES spectrum of QSO 1243+3047 calibrated using the Kast K99 spectrum of QSO 1243+3047, HKSUM was

calibrated using the mean of all five Kast spectra and HESI was calibrated using the ESI spectrum of QSO 1243+3047.

We also made a spectrum, HH, which we calibrated using a HIRES spectrum of a standard star. This HH calibration is not typical of the accuracy that we usually obtain, but rather it is the best that we could obtain with our spectra. We made many calibrations using different HIRES integrations of standard stars, and we show the calibration that had the smoothest order joins. This HH calibration contrasts with the calibrations of the stars that we showed in Fig. 3 that did not work as well.

In Figure 15, we show the ratios of HIRES spectra calibrated in these different ways. The top panel shows HK99 spectra divided by HESI. There is a 7% difference across the wavelength region shown. The HK01 differs from HESI by 5% at most, while the HKSUM calibration differs from HESI by 4%. The calibrations HH and HESI differ the least – only 3% – but show the largest jumps at order joins, e.g. near 4325 Å. The four gray bands of Figure 15 show the wavelength overlaps between the HIRES orders. We show three complete orders and two partial ones.

We show the wavelength region centered on the strong Ly α lines that we have use to measure the H I column density that contributes to a D/H measurement. This Ly α line has damping wings that absorb approximately 1% of the flux near 4233 and 4340 Å and hence accurate flux calibration of this region helps us measure the column density, although most information comes from 20 Å on either side of the line center.

The differences between the calibrations have three origins. The largest differences, which are on the largest scales, come from the differences between the K99, K01 and ESI spectra. Other differences, especially near the order joins, are related to the fitting of the CR, and are sensitive to the signal to noise ratio in the Kast and ESI spectra. A third type of difference occurs from pixel to pixel, and comes from the rejection of deviant pixels from among the 8 HIRES integrations. The CR fits are smooth curves, and the ratios would also be smooth were it not for differences in the pixels which are rejected when we took the sum of the 8 integrations. The numerous small 1 – 2% deviations arise when a pixel is not used from one integration or another. The size of these deviations is given by the signal to noise ratio of the individual integrations. The noise increases in the strong absorption lines where we are dividing two HIRES spectra, each of which has low signal to noise noise. Trends that are seen in more than one panel may come from differences of the ESI spectrum from the others.

We do not know which of the spectra is the more accurate. All of the spectra used in Figure 15 were calibrated with CR spectra that were fit order by order. We found that the

2-dimensional fits to the CR, like that shown in Figure 13, slightly reduced the deviations near the order joins.

9. Discussion of the Accuracy of the Flux Calibration

Many factors contribute to the errors in the relative flux calibration, including:

- Errors in the flux reported for the standard star.
- Errors in our spectra of the standard star and reference. Common error sources include extinction and absorption in the Earth’s atmosphere, slit losses that depend on wavelength, a dichroic in the spectrograph, variation of the target, variation with wavelength of the proportion of the flux extracted, and the S/N of the spectra.
- Errors calculating the response function that we use to calibrate the reference spectrum. Errors occur matching the resolution and wavelength scales of our spectrum of the standard to the published flux information. Such errors are especially conspicuous near absorption lines in the standard.
- Errors in the preparation of the HIRES spectrum, including the bias subtraction, flat field division and extraction.
- Errors applying the flux calibration to HIRES spectrum, including wavelength shifts, resolution differences, the signal to noise ratio of the HIRES spectrum and fitting the CR.

We have found that many of these factors can produce 1 – 10% errors in flux calibration, but it is difficult to assign typical values for these errors.

The size of the error in the relative flux calibration depends on the wavelength and the wavelength range. We do not include errors from the CR in the usual error array because the CR errors are correlated over many pixels. In this paper we have concentrated on scales of a few orders, or approximately 120 Å that are most relevant to our work on D/H. We have paid much less attention to the relative flux calibration on larger scales that are dominated by a different set of factors, such as the extinction at the time of observation. We expect errors due to extinction to monotonically increase with scale in our reference spectrum.

An indication of the accuracy we have attained in relative flux calibration is given in Figure 14. We compare three spectra of the flux standard star Feige 34: a HIRES spectrum that we flux calibrated using a Kast spectrum as the reference, the Kast reference spectrum,

and STIS a spectrum. The Kast and STIS spectra are those shown in Figure 6. The STIS spectrum was not used in the calibration, except to provide the normalization of the Kast spectrum across the range 3200 – 4450 Å. We used a one-dimensional 4th order polynomial to fit the CR. In the wavelength region shown, the HIRES spectrum differs from its reference by at most 2.5%, except near the absorption line, and typically < 1%. At wavelengths 3400 – 3800 Å, where the signal to noise ratio is lower, the differences are twice as large. The differences correlate on scales > 5 Å. The flux in different HIRES orders joins smoothly, with no unusual structure. The remaining differences of the HIRES and STIS spectra come from the deviation of the Kast spectrum from the STIS, shown in Figure 14. This comparison demonstrates that the method can give errors of < 1% in the relative flux over approximately 200 Å. For Feige 34 the accuracy of the flux calibration was limited by the accuracy of the reference, and not by the method itself.

10. SUMMARY

We found that the distribution of the signal recorded in HIRES integrations differs from integration to integration. We do not have a complete explanation for this behavior, although varying vignetting and inadequate extraction may be involved. We found that these differences persist even when the instrument is apparently unchanged. These changes mean that the usual methods of flux calibration are inadequate.

The methods we have described for applying relative flux calibration to a HIRES spectrum use three spectra: the HIRES spectrum of the target that we wish to calibrate, and Kast spectra of both the target and a flux standard star. We use the latter to get the Kast response and calibrate the Kast spectrum of the target that we name the reference spectrum. We use reference spectrum to impose flux calibration on the HIRES target spectrum.

This method has three advantages. First, we can calibrate HIRES when normal calibrations using standard stars observed with HIRES alone are inadequate. Second, we can correct many types of error in the HIRES spectrum, including those from varying vignetting and inadequate extraction. Finally, we can obtain all the calibration spectra at a different time and on a different telescope.

The error in relative flux calibration, and the solution that we describe, could apply to any spectrum with inadequate relative flux calibration, whether from an unstable spectrograph or from inadequate extraction. Vignetting could vary in any spectrograph that was unstable. Instability could involve an optical misalignment, as with HIRES. Variable vignetting would be harder to recognize in a first order spectrum because we expect the

largest changes near the largest field angles, but there is only one spectrum to show this change, and flux calibration is often harder near the ends of a single spectrum, for other reasons.

11. Acknowledgments

This work was funded in part by grant NAG5-9224 and by NSF grant AST-9900842 and AST-0098731. The spectra were obtained from the Lick and the W.M. Keck observatories. The W.M. Keck observatory is managed by a partnership among the University of California, Caltech and NASA. We are grateful to Steve Vogt, the PI for the Keck HIRES instrument that enabled our work on D/H, for many invaluable discussions, along with Tom Barlow, who developed the MAKEE extraction software package. We also thank Wako Aoki and Kunio Noguchi for discussions of the HDS echelle spectrograph, and the W.M. Keck Observatory staff and the Lick Observatory staff.

A. Appendix A: Choice of Standard Star

We used the calibrations of the flux in stars based on STIS spectra (Bohlin, Dickinson, & Calzetti 2001). In Figure 16 we see that the STIS spectra do not show the wiggles at 3200-3850 Å that are present in the Oke (1990) spectrum of G191 B2B. This and other Oke spectra are widely used by default in the reduction packages IRAF and MIDAS. The differences between the Oke (1990) and STIS spectra can reach several percent, larger than our random photon noise. Based on the lack of features in the spectrum and the STIS data quality, we preferred the following stars for UV flux calibration near 3200 Å: G191 B2B, BD+28 4211, Feige 110, and Feige 34. For G191 B2B we have the additional choice of using a model spectrum given by Bohlin et al. (2001). This model spectrum fits their STIS spectra to within 0.7 % in the continuum (Bohlin 2000), and it simplifies flux calibration because it has full resolution.

We used the entire STIS spectrum for flux calibration, including the broad Balmer absorption lines. The Oke (1990) paper provides AB magnitudes at discrete continuum points in 5-50 Å intervals. These points skip the Balmer absorption lines, but we can not do this, because we then have insufficient information to calibrate several echelle orders, each of which is only 30-60 Å long.

Our use of the flux calibration information near the Balmer lines can help us avoid significant errors. In Figure 17 we show a spectrum from ESI echellette order 15 that has

its sensitivity peak around 4350 Å that coincides with Balmer γ line, 4341.68 Å. QSO 1243+3047 (Kirkman et al. 2003) happens to have its Ly α emission at 4330 Å. In an early flux calibration of this order, poor interpolation across this Balmer line had led us to make an 8% calibration error that was three times the random error.

B. Appendix B: HIRES Image Rotator

The vignetting in HIRES depends on whether or not the image rotator is used, and on the mode in which the rotator is used.

HIRES is fixed to the Nasmyth platform of the Keck-I telescope with its slit approximately parallel to the horizon. When we look at the image of the sky on the HIRES slit, we see that the vertical direction in this image rotates at a rate given by the elevation (EL) of the telescope. This is because telescope is rotating in EL while HIRES is fixed. If the telescope is pointing at the horizon, and looking at an arrow in the sky that is pointing towards the zenith, the image of this arrow on the slit plane is also pointing towards the vertical, which is perpendicular to the length of the slit. As the telescope moves to higher EL, the arrow rotates until it is aligned along the slit when the telescope is pointing to the zenith.

The HIRES image rotator allows us to rotate the image of the sky on the slit plane in any way we like. We installed an image rotator in HIRES in late 1996. This is a large quartz prism that sits in front of the HIRES slit. The light from the Keck-I telescope tertiary mirror undergoes three total internal reflections in the prism before coming to a focus on the slit plane. The prism can rotate continuously in either direction about the axis of the beam that converges on the center of the slit. The prism is aligned so that the image of a star on the center of the slit moves by under 0.5 arc seconds when the prism is moved in or out of the beam, and when the prism is rotated. The prism can be spun rapidly to demonstrate this alignment. The prism does not vignette any of the beam that lands within 60 arc seconds of the center of the slit.

The image rotator has two main modes of operation: Position Angle and Vertical Angle. The position angle mode is used when we wish to keep two stars in the slit, where as the vertical angle mode is used to keep the vertical direction in the sky parallel with the slit, as a surrogate for an atmospheric dispersion compensator. When the image rotator was used in Vertical mode, the position angle along the slit is the parallactic angle, and this varies as we track a target. The parallactic angle is measured at the target, from the North Celestial Pole to the Zenith, in the direction from North via East. The parallactic angle is fixed for

a given elevation and azimuth in the sky, but it changes when we track a target across the sky.

HIRES spectra are hard to flux calibrate in part because the vignetting can change by 10% from spectrum to spectrum. The vignetting changes because there is a known misalignment between the beam coming from tertiary mirror and the HIRES optical axis. When HIRES was installed, the center of the Keck telescope pupil was measured to be approximately 9 mm away from the collimator center, which corresponds to a beam misalignment of 7.4 arcminute. If a star is held at one position on the HIRES slit, the axis of the beam entering HIRES will rotate around the HIRES optical axis at a rate given by any change in the position angle of the sky image on the slit. If the position angle moves through 360 degrees, the axis of the beam entering HIRES follows the surface of a cone with an apex angle of approximately 14.8 arcminutes. Steve Vogt used ray tracing to find that this rotation causes the vignetting to vary by approximately 10%, depending on the angle. The vignetting occurs due to a dewar which forms a central obstruction in the beam near the camera's prime focus.

REFERENCES

- Aoki, W. 2002, <http://www.subarutelescope.org/Observing/Instruments/HDS/index.html>
- Barlow, T. A. & Sargent, W. L. W. 1997, *AJ*, 113, 136
- Bigelow, B. C. & Nelson, J. E. 1998, in *Proc. SPIE Vol. 3355*, p. 164-174, *Optical Astronomical Instrumentation*, Sandro D'Odorico; Ed., Vol. 3355, 164–174
- Bohlin, R. C. 2000, *AJ*, 120, 437
- Bohlin, R. C., Dickinson, M. E., & Calzetti, D. 2001, *AJ*, 122, 2118
- Burki, G., Rufener, F., Burnet, M., Richard, C., Blecha, A., & Bratschi, P. 1995, *A&AS*, 112, 383
- Burles, S. & Tytler, D. 1997, *AJ*, 114, 1330
- . 1998, *ApJ*, 507, 732
- Clayton, M. 1996, <http://starlink.rl.ac.uk/star/docs/sg9.htx/sg9.html>
- Dekker, H., D'Odorico, S., Kaufer, A., Delabre, B., & Kotzlowski, H. 2000, in *Proc. SPIE Vol. 4008*, p. 534-545, *Optical and IR Telescope Instrumentation and Detectors*, Masanori Iye; Alan F. Moorwood; Eds., Vol. 4008, 534–545

- Diego, F., Charalambous, A., Fish, A. C., & Walker, D. D. 1990, in Instrumentation in astronomy VII; Proceedings of the Meeting, Tucson, AZ, Feb. 13-17, 1990 (A91-29601 11-35). Bellingham, WA, Society of Photo-Optical Instrumentation Engineers, 1990, p. 562-576. Anglo-Australian Observatory-supported research., Vol. 1235, 562–576
- Epps, H. W. & Miller, J. S. 1998, in Proc. SPIE Vol. 3355, p. 48-58, Optical Astronomical Instrumentation, Sandro D’Odorico; Ed., Vol. 3355, 48–58
- Kirkman, D., Tytler, D., Suzuki, N., O’Meara, J. M., & Lubin, D. 2003, ApJSubmitted, astro-ph/0302006
- Massey, P., Valdes, F., & Barnes, J. 1992, <http://iraf.noao.edu/docs/spectra.html>
- McLean, I. S., Becklin, E. E., Bendiksen, O., Brims, G., Canfield, J., Figer, D. F., Graham, J. R., Hare, J., Lacayanga, F., Larkin, J. E., Larson, S. B., Levenson, N., Magnone, N., Teplitz, H., & Wong, W. 1998, in Proc. SPIE Vol. 3354, p. 566-578, Infrared Astronomical Instrumentation, Albert M. Fowler; Ed., Vol. 3354, 566–578
- Noguchi, K., Ando, H., Izumiura, H., Kawanomoto, S., Tanaka, W., & Aoki, W. 1998, in Proc. SPIE Vol. 3355, p. 354-362, Optical Astronomical Instrumentation, Sandro D’Odorico; Ed., Vol. 3355, 354–362
- Oke, J. B. 1990, AJ, 99, 1621
- O’Meara, J. M., Tytler, D., Kirkman, D., Suzuki, N., Prochaska, J. X., Lubin, D., & Wolfe, A. M. 2001, ApJ, 552, 718
- Schachter, J. 1991, PASP, 103, 457
- Schroeder, D. J. 1987, Astronomical Optics (San Diego: Academic Press, 1987)
- Sheinis, A. I., Miller, J. S., Bolte, M., & Sutin, B. M. 2000, in Proc. SPIE Vol. 4008, p. 522-533, Optical and IR Telescope Instrumentation and Detectors, Masanori Iye; Alan F. Moorwood; Eds., Vol. 4008, 522–533
- Tull, R. G. 1998, in Proc. SPIE Vol. 3355, p. 387-398, Optical Astronomical Instrumentation, Sandro D’Odorico; Ed., Vol. 3355, 387–398
- Vogt, S. S. 1987, PASP, 99, 1214
- Vogt, S. S., Allen, S. L., Bigelow, B. C., Bresee, L., Brown, B., Cantrall, T., Conrad, A., Couture, M., Delaney, C., Epps, H. W., Hilyard, D., Hilyard, D. F., Horn, E., Jern, N., Kanto, D., Keane, M. J., Kibrick, R. I., Lewis, J. W., Osborne, J., Pardeilhan,

G. H., Pfister, T., Ricketts, T., Robinson, L. B., Stover, R. J., Tucker, D., Ward, J., & Wei, M. Z. 1994, in Proc. SPIE Instrumentation in Astronomy VIII, David L. Crawford; Eric R. Craine; Eds., Volume 2198, p. 362, Vol. 2198, 362+

Willmarth, D. & Barnes, J. 1994, <http://iraf.noao.edu/docs/spectra.html>

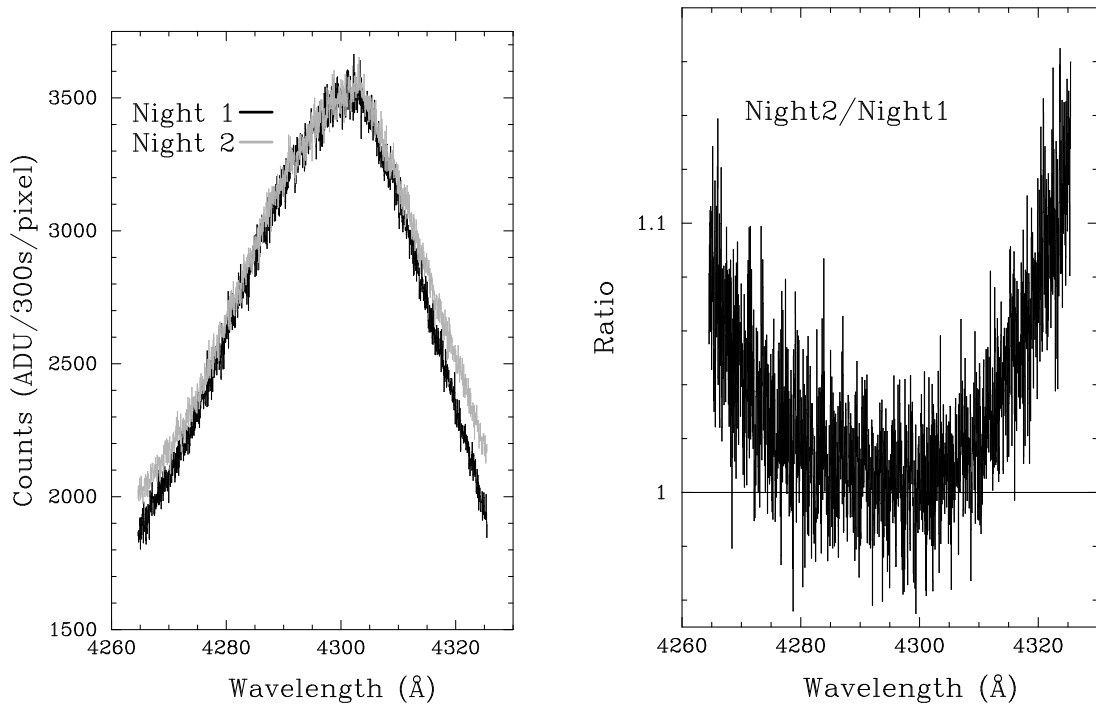


Fig. 1.— Two 300 second integrations of the star G191-B2B taken with near identical HIRES setups on consecutive nights: 19 (solid) and 20 (light) September, 2000. The right panel shows the ratio of the two. These spectra were taken with the C5 dekker (1.14 arcsec slit), and the image rotator was set to align the sky vertical along the slit. The September 19 integration had sidereal time $ST = 05:16:48$ hours, telescope elevation $EL = 56.96$ degrees, and image rotator physical angle, as measured looking at the prism, of $IROT2ANG = 195.9357$ degrees. For September 20th we had $ST = 05:02:24$, $EL = 57.03$ degrees and $IROT2ANG = 195.8646$. The September 20th spectrum was multiplied by 1.06 to give similar counts to the other near 4300 \AA to correct for differences in the atmospheric transparency, seeing and the loss of light at the slit.

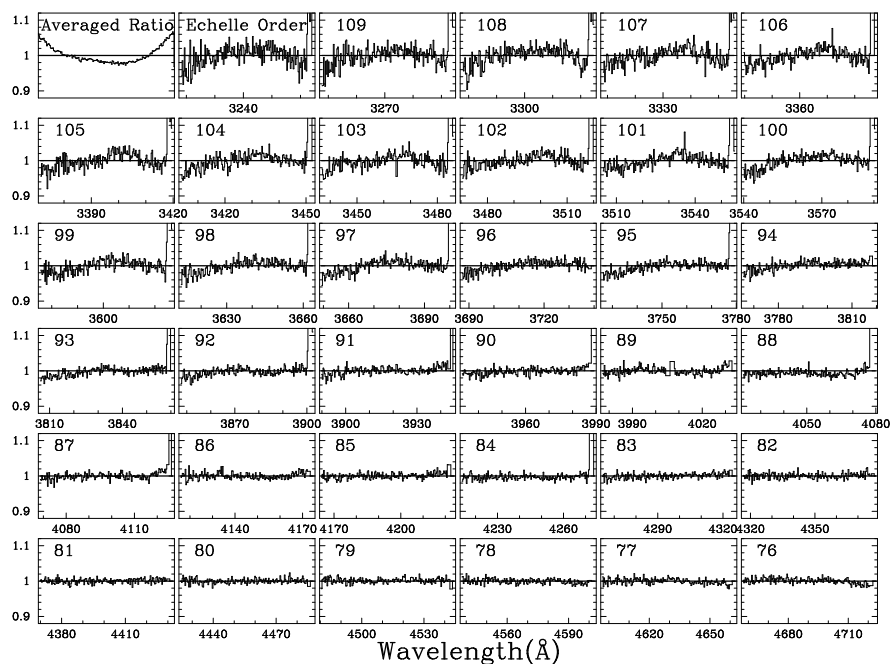


Fig. 2.— The ratio of the two spectra shown in Fig. 1, divided by average ratio from the ten orders with the largest wavelengths. We show this average in the top left panel, and other panels each show one HIRES order. We show the full amount of each order that fell on the CCD, which includes some wavelength overlap between adjacent orders. We have re-binned the original 2048 pixels into 205 pixels for presentation.

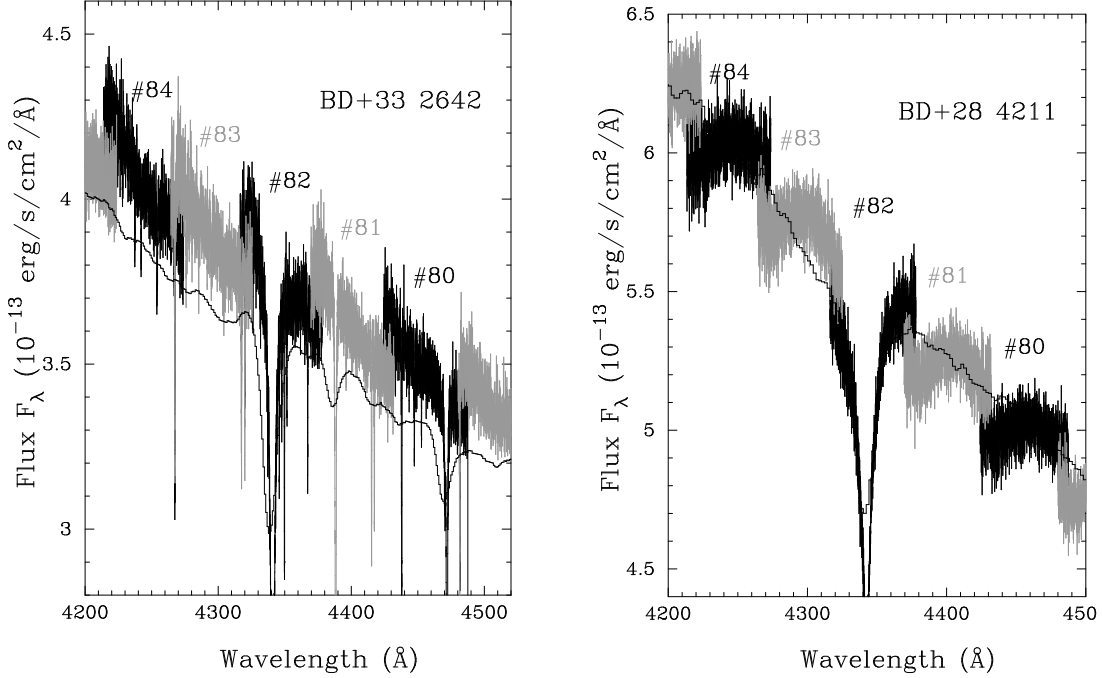


Fig. 3.— Hires spectra of stars that we flux calibrated in the usual manner. In both cases we see large flux calibration errors. In other cases we can obtain smaller errors. Left, Hires integration of star BD+33 2642. We determined the response function of Hires by comparing a Hires spectrum of G191-B2B, taken on the same night (September 19, 2000), to a model spectrum with known flux (Appendix A). The continuous line shows a lower resolution HST FOS spectrum of BD+33 2642. We may adjust the Hires spectrum vertically to account for slit losses. The right panel is the same, but for a Hires integration of BD+28 4211 obtained October 10, 1999, calibrated with a Hires spectrum of G191-B2B, taken on the same night. The continuous line is a STIS spectrum of BD+28 4211.

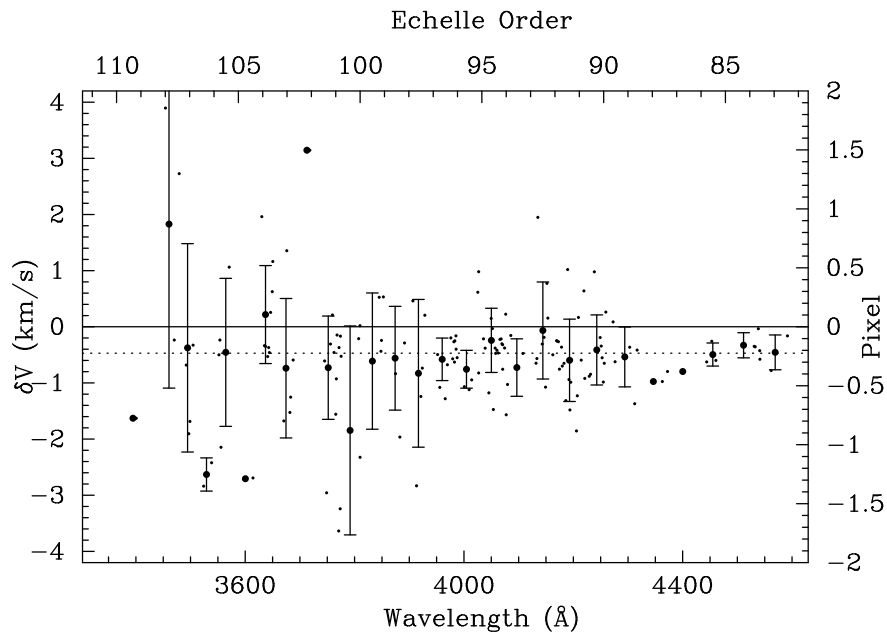


Fig. 4.— The wavelength shifts measured between two consecutive HIRES integrations for QSO 1243+3047, both taken on March 13, 2000. The small points show shifts measured by cross-correlating blocks of approximately 20 pixels that contain an absorption line. The larger points show the mean shift per order, and the vertical bars show $\pm 1\sigma$ from the distribution of the measurements in that order. The dotted line shows the mean shift between the two integrations.

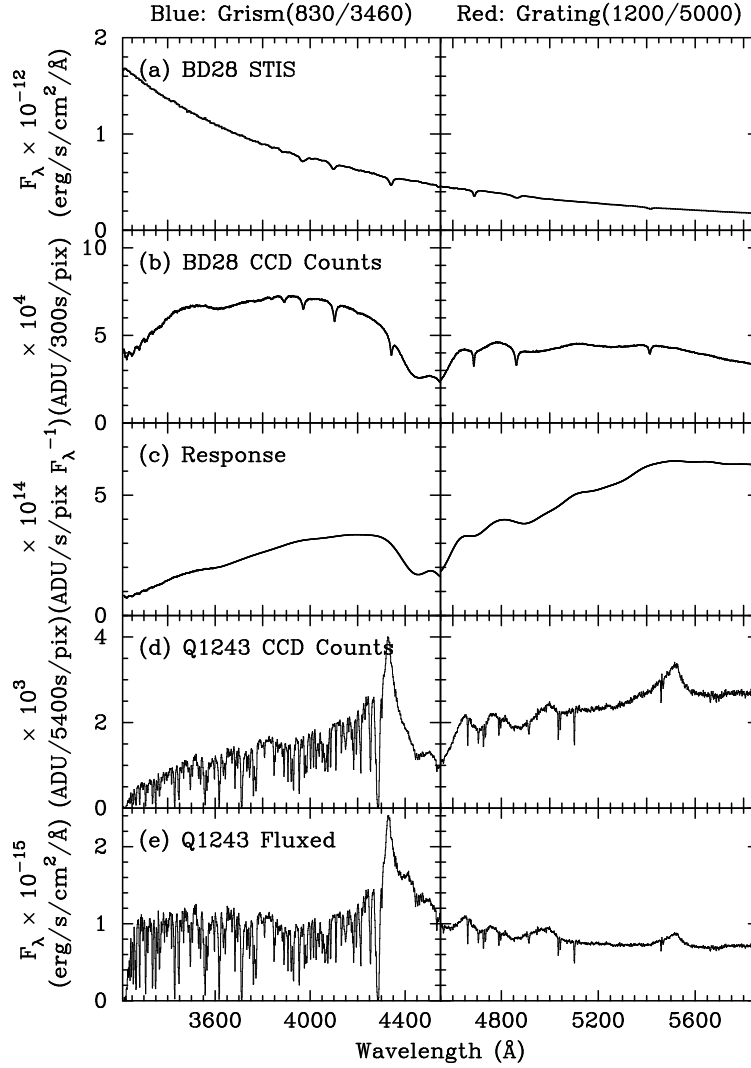


Fig. 5.— Steps in the calibration of the flux in a Kast spectrum. Panel (a) shows the STIS spectrum of star BD+28 4211. Panel (b) shows the raw counts recorded in two simultaneous Kast integrations, one with the blue camera (left) and one with the red camera (right). We do not show the wavelength overlap on either side of the central wavelength of the dichroic beam splitter (called d46), which we show with the vertical line near 4450 Å. We had moved the “x-stage” that holds the CCD of the blue camera of Kast to sample wavelengths well beyond the peak of the Ly α emission line. Panel (c) shows the response function (b)/(a), and panel (d) shows the raw counts in one 5400 second integration on QSO 1243+3047. Panel (e) shows the flux calibrated spectrum, (d)/(c).

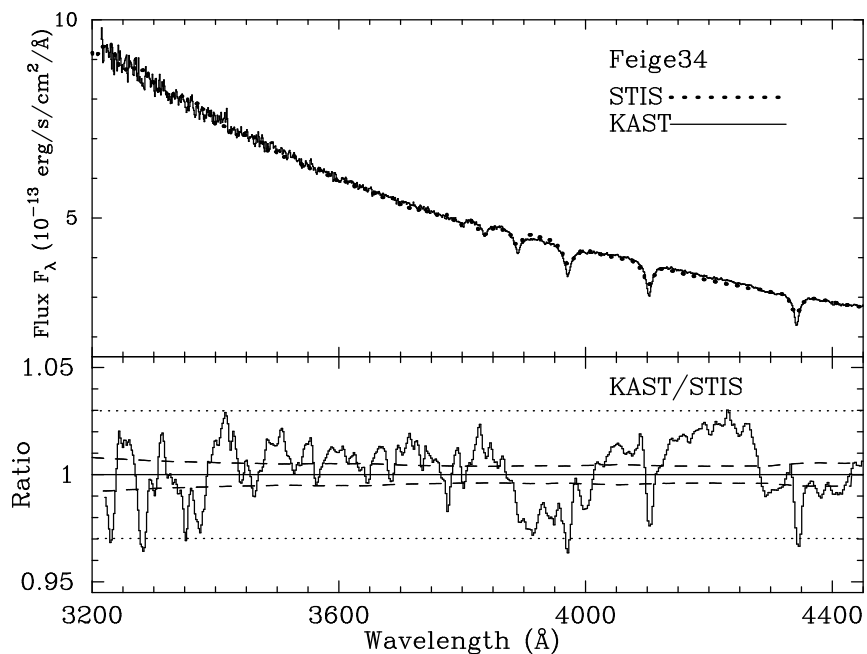


Fig. 6.— Top Panel: Two spectra of the star Feige 34, one from STIS (solid line, Bohlin et al. 2001), and the other a Kast spectrum that we have flux calibrated (dotted). We calibrated the Kast spectrum with Kast spectrum of the star BD+28 4211. We also normalized the Kast spectrum to have the same mean flux as the STIS spectrum to adjust for slit losses. Bottom Panel: Ratio of the two spectra in the top panel. The dotted line is the error for the STIS spectrum (approximately 1% random and 3% systematic), and the dashed line is the random error from the photon noise in the Kast spectrum. These errors are for 2 Å pixels.

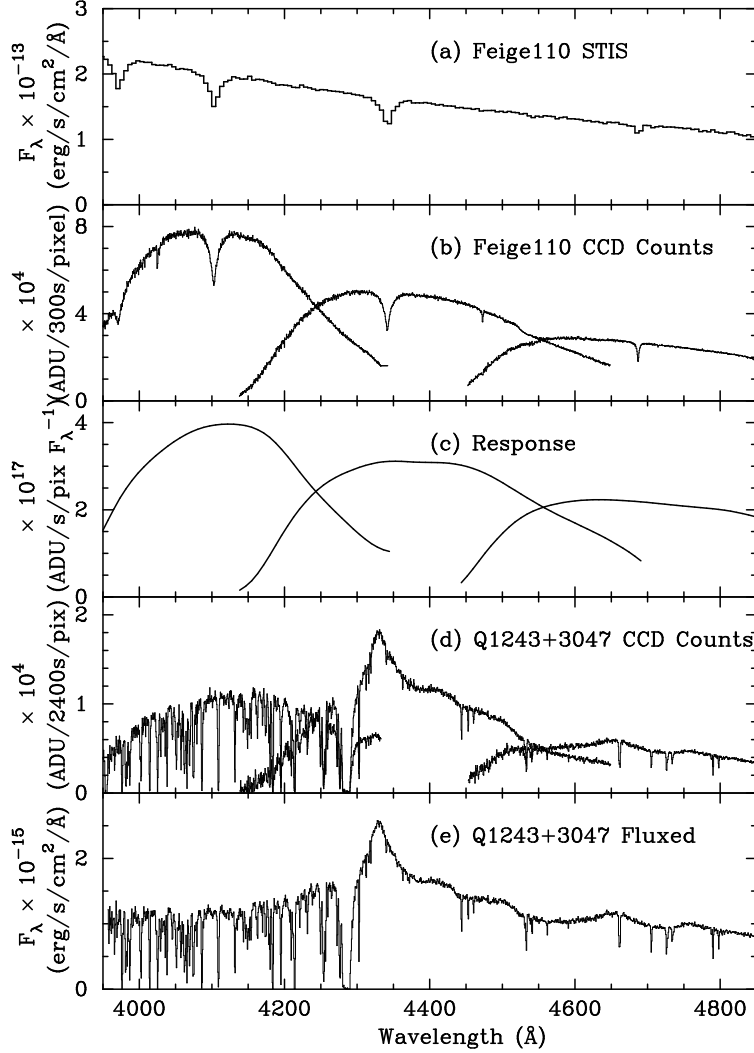


Fig. 7.— Steps in the flux calibration of an ESI integration of QSO 1243+3047 using an ESI spectrum of the star Feige 110 obtained on the same night. We show only 3 of the 10 ESI orders. Panel (a) at the top shows the STIS flux calibrated spectrum of star Feige 110. Panel (b) shows the raw CCD counts from an ESI spectrum of this star. Panel (c) shows the smoothed ratio (b)/(a) that is the response function of ESI. Panel (d) shows the raw counts from an integration of QSO 1243+3047, and panel (e) shows the same spectrum after relative flux calibration.

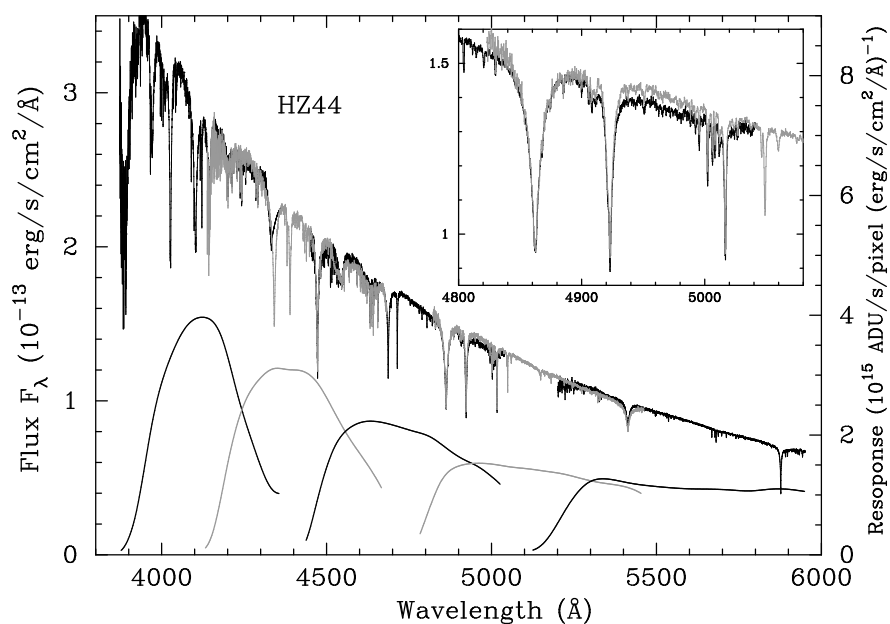


Fig. 8.— Demonstration of the errors in the flux calibration of an ESI spectrum of the star HZ44. The middle traces show the ESI orders after flux calibration using an ESI spectrum of star Feige 110. The lower smooth curves show the response function of these ESI orders. Here we use the usual flux calibration methods. The insert in the upper right is an enlargement of 4800 – 5100 Å that clearly shows that adjacent orders differ.

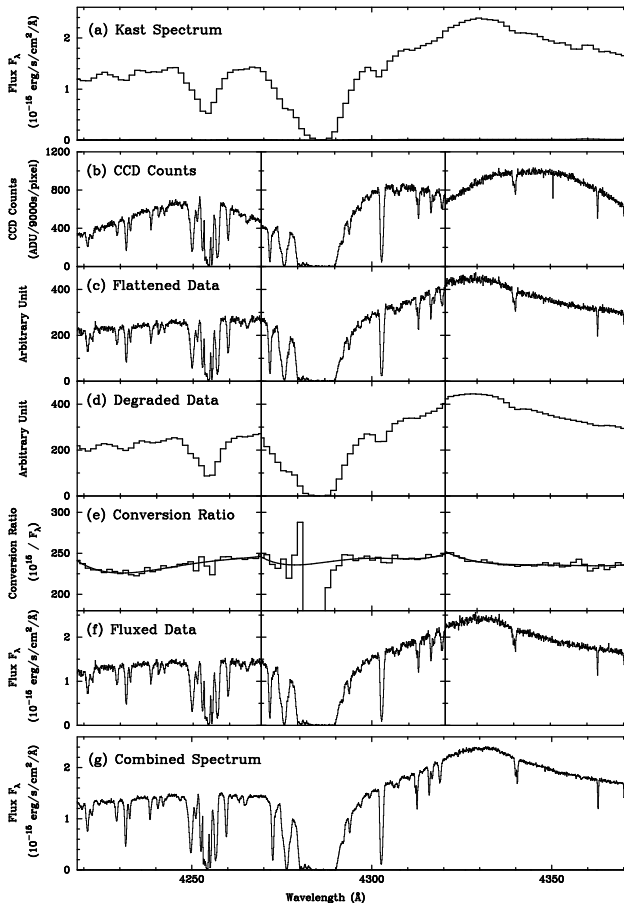


Fig. 9.— Illustration of the steps taken to apply relative flux to HIRES spectra of QSO 1243+3047 using Kast spectra of the same QSO. Panel (a) shows a flux calibrated Kast spectrum. It has been shifted in wavelength to match the HIRES wavelengths. Panel (b) shows the CCD counts recorded in the three HIRES orders that cover these wavelengths. This is a single HIRES integration, and the orders overlap in wavelength, although we do not show this here. Panel (c) shows the extracted HIRES orders that have been “flattened” by dividing by the flat field. This is the Flux-name.fits file that is the usual output from MAKEE. Panel (d) is shows the spectra from panel (c) after smoothing by a Gaussian filter to match the spectral resolution of the Kast spectrum in panel (a). The HIRES spectrum has been re-binned onto the Kast pixels. Panel (e) shows the ratio (d)/(a) that we call the conversion ratio. It has values at the Kast pixels, and two values at the wavelengths that appear in two HIRES orders. The smooth curves are low order fits to the pixels that sample the conversion ratio. Panel (f) is (c)/(e), the flux calibrated HIRES spectra. Notice that the jump in the HIRES flux at the order join near 4320 Å in panels (b), (c) and (d) is detected by the conversion ratio in (e) and corrected in (f). Panel (g) shows the sum of 8 HIRES integrations, each of which is corrected individually in the same manner. The order joins are not apparent. We do not plot most pixels in the high resolution spectra, to reduce the file size.

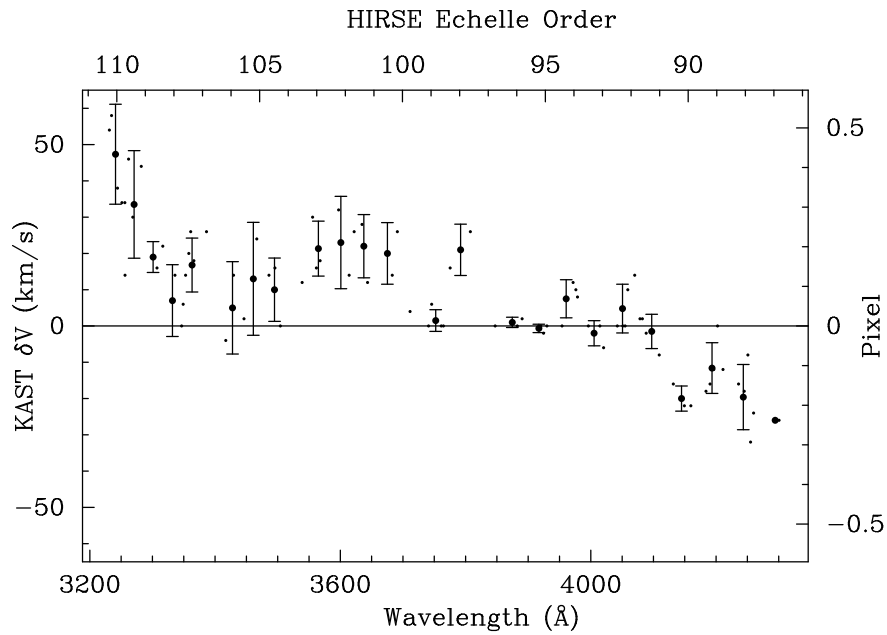


Fig. 10.— Shifts in the wavelength scale of a spectrum of QSO 1243+3047 from the Kast spectrograph measured relative to a HIRES spectrum of the same QSO. Each dot shows the shift measured by cross-correlating a region of spectrum that contains an absorption line. The bars show means of these dots, taken over the individual HIRES orders. We obtain similar shifts when we cross-correlate over complete HIRES orders. The sampling pixel size is 107.1 km s^{-1} .

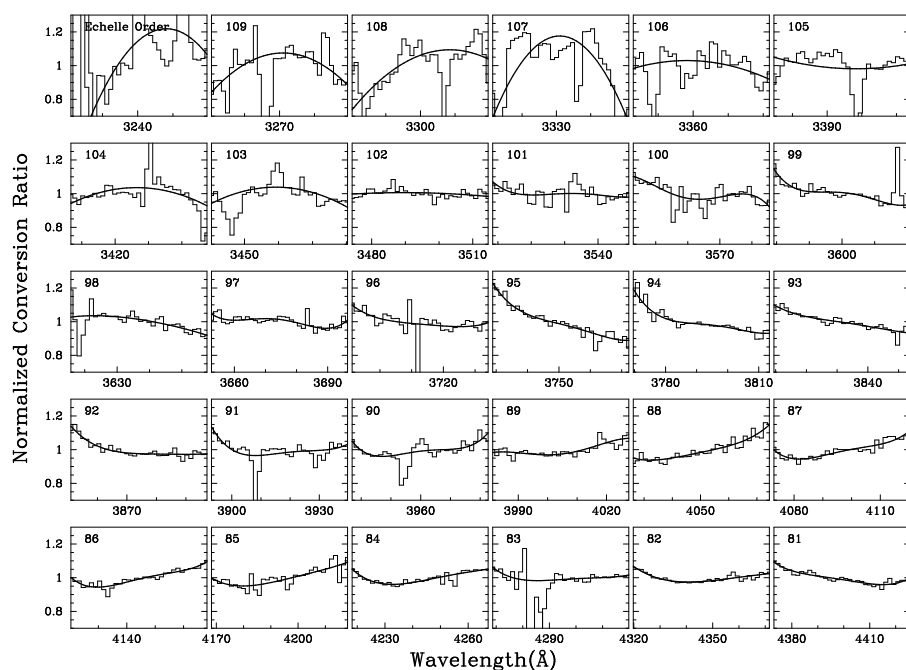


Fig. 11.— Conversion ratio for the 8100 second HIRES integration of QSO 1243+3047 taken April 4, 1999. The relative flux calibration uses a Kast spectrum from 2001. The mean level of the CR in each order has been normalized for the plot. The pixels sizes are from the Kast spectrum, and the curves show 4th order Chebyshev polynomial fits to each order.

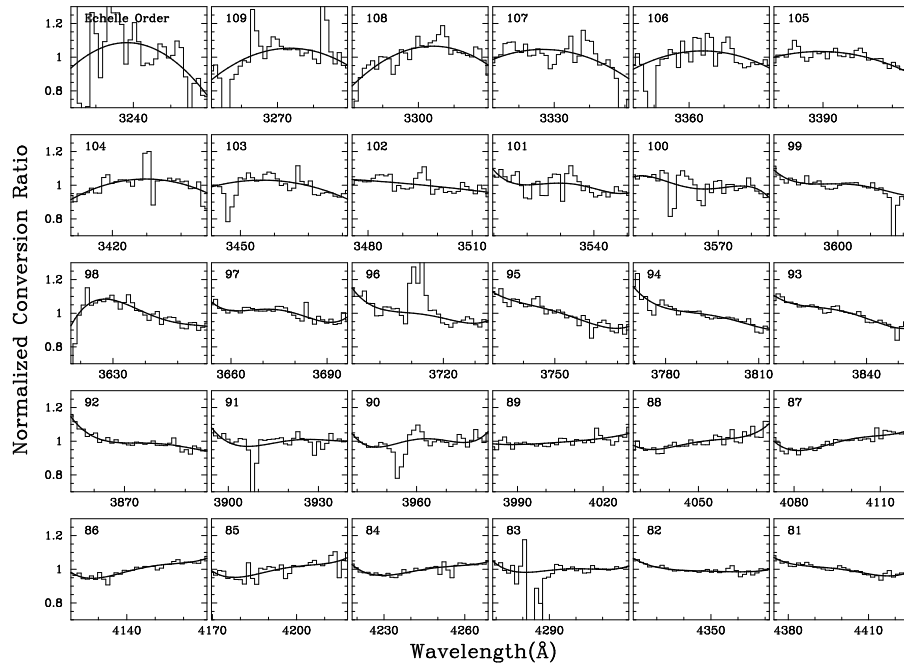


Fig. 12.— As Fig. 11, but for a 7200 second HIRES integration taken 11 months later on March 14, 2000.

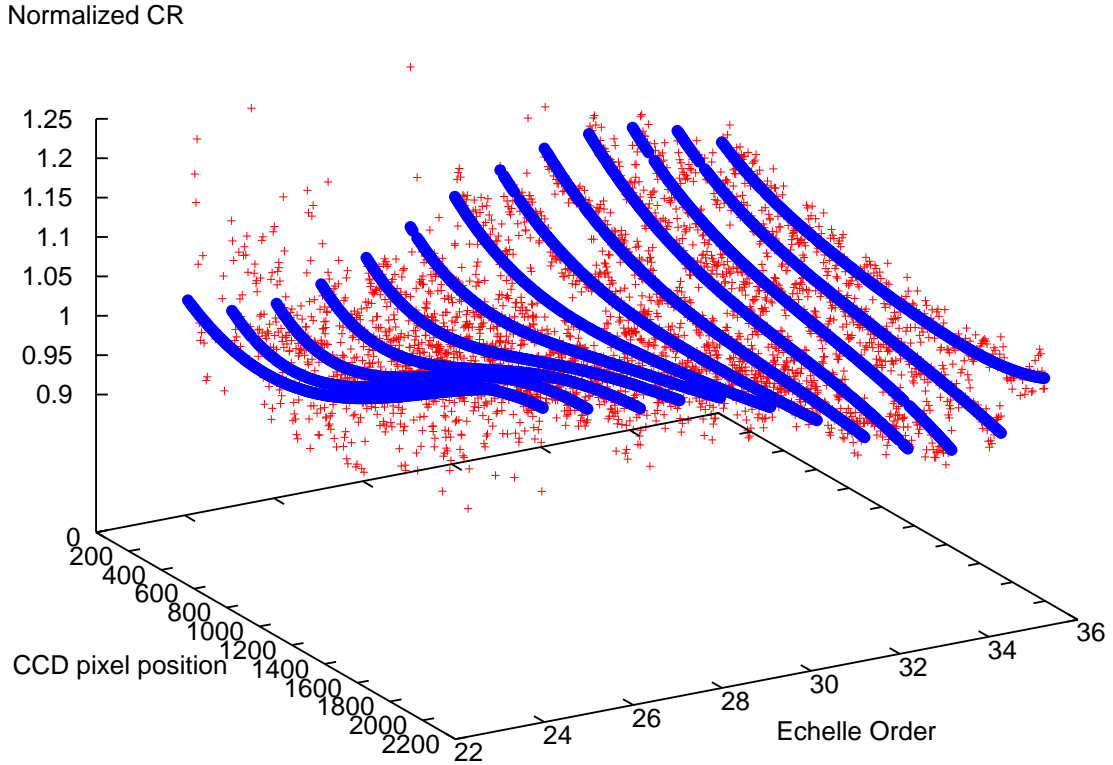


Fig. 13.— The conversion ratio for a HIRES integration of QSO 1243+3047 fitted with a 2-dimensional Chebyshev polynomial. Each small plus sign shows the CR value in a pixel of the reference spectrum from ESI. The CR values are shown elevated above a plane that approximates the HIRES CCD. The axis “CCD pixel position” is the pixel along the direction of a HIRES order, with wavelength increasing to higher numbers. The axis “Echelle Order” is encoded such that 113 - the number given is the HIRES order. The orders are shown parallel to each other and with equal spacing. The vertical height of a plus sign shows the CR in that ESI pixel, and the other two coordinates show the location of the HIRES pixel with a similar wavelength. The S/N in the ESI spectrum increases with wavelength, to the left. The CR have been normalized to have a mean CR = 1 in the middle 20% of each HIRES order. Prior to this, the CR varied systematically by approximately a factor of two. The thick curves show the Chebyshev polynomial along each order. These polynomials are constrained to 4th order in both the CCD pixel and echelle order directions.

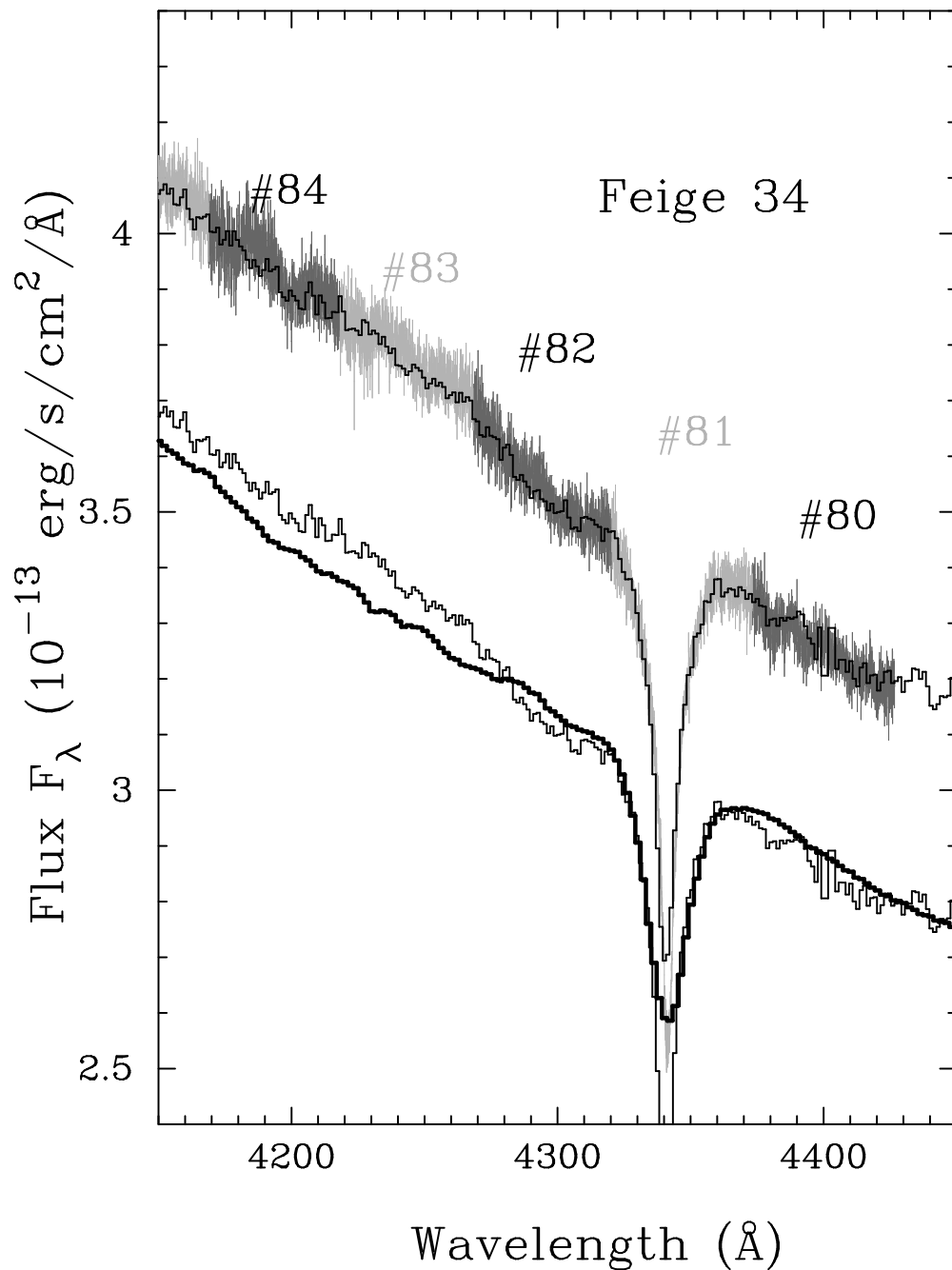


Fig. 14.— Spectra of star Feige 34 with relative flux calibration. The lower two spectra are from STIS (heavy line) and Kast (thin line), both from Fig. 6. The upper two spectra, displaced vertically by the same amount for clarity, are the same Kast reference spectrum and five and a half orders of a HIRES spectrum (faint trace with many pixels, darker in even numbered orders).

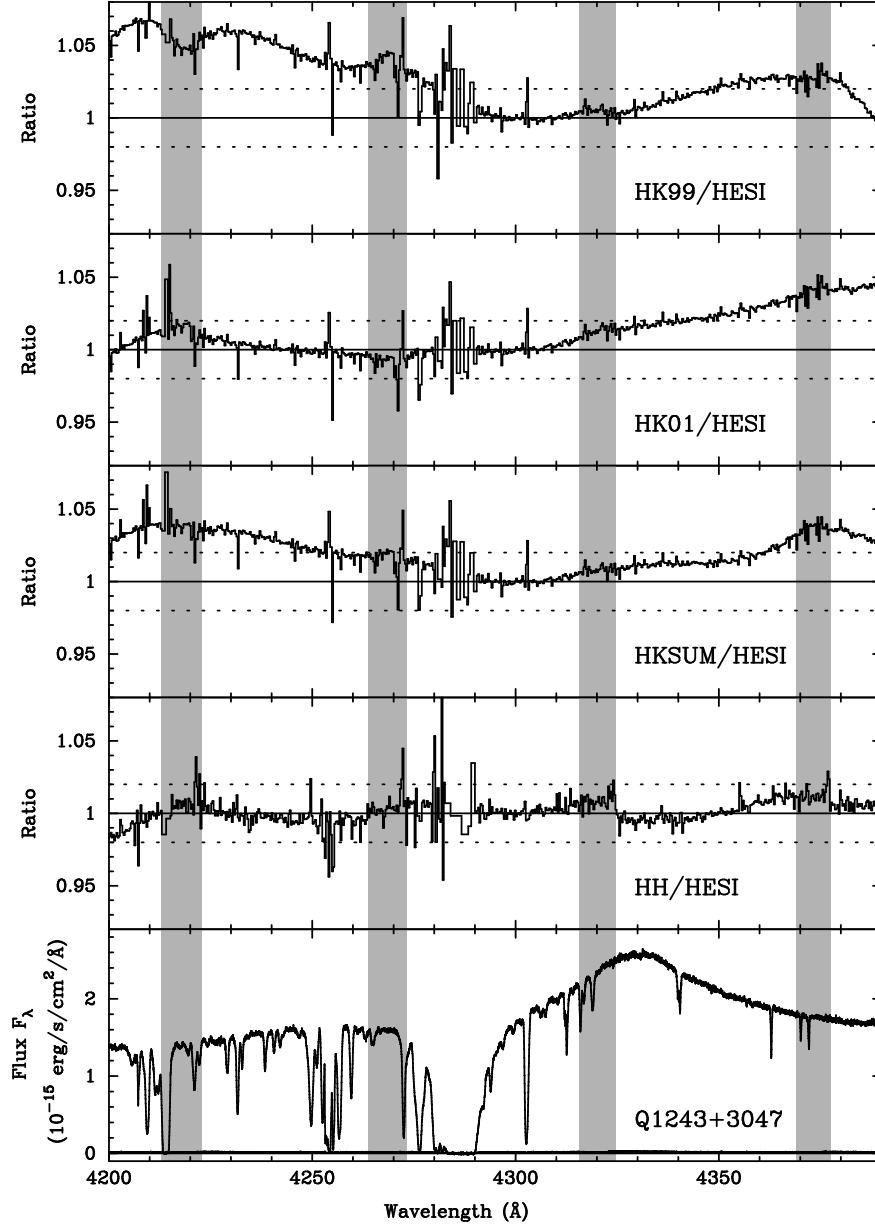


Fig. 15.— Ratios of the flux in different summations of the 8 HIRES integrations of QSO 1243+3047 that we have calibrated using different spectra. HK99, HK01 and HKSUM were all calibrated with Kast spectra, while HESI and HH are HIRES spectra calibrated using ESI spectra and a HIRES spectrum of a flux standard. Each of the top 4 panels shows the ratio of two HIRES spectra, each one of which looks similar to that shown in the bottom panel. The vertical bands show the wavelengths where the orders overlap. We do not plot most pixels, to reduce the file size. If we had plotted all pixels, the noise near the few strongest absorption lines would be much more conspicuous, and in each 10 Å interval we would see 1 – 20 fluctuations of 1 – 2%. We also do not plot pixels that have negative flux, because of the random noise in the sky subtraction.

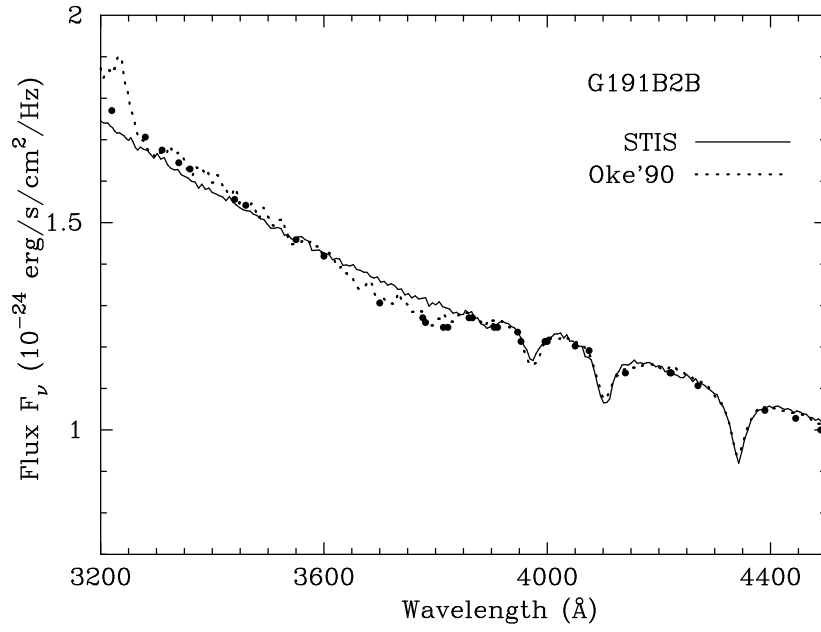


Fig. 16.— Flux calibrated spectra of the star G191-B2B. The continuous, wobbly line is a STIS spectrum from Bohlin (2000). The dotted line and points are from Oke (1990).

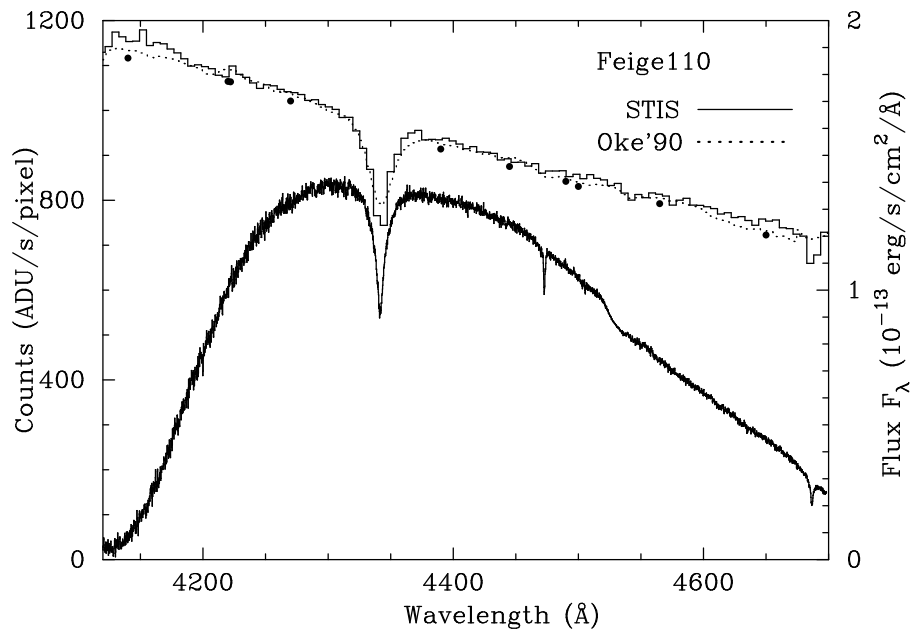


Fig. 17.— Spectra of the flux standard star Feige 110. The lowest trace shows the signal recorded in one ESI order. The dotted line shows the flux reported by Oke (1990) and the points show the flux values that he recommended to minimize sensitivity to spectral resolution. The STIS spectrum from (Bohlin, Dickinson, & Calzetti 2001) is shown by the continuous trace comprising pixels that are easy to see on the plot.